

# Machine learning-based identification of H&E-derived morphologic features associated with CD8+ T cell immune exclusion

Yanchao Wang<sup>1</sup>, Fredrick D. Gootkind<sup>1</sup>, Florent Peyraud<sup>2</sup>, Jean-Philippe Guégan<sup>3</sup>, Antoine Italiano<sup>2</sup>, G. Travis Clifton<sup>1</sup>, Laura A. Dillon<sup>1</sup>, Xinwei Sher<sup>1</sup>

<sup>1</sup>Incendia Therapeutics, Boston, MA, USA; <sup>2</sup>Early Phase Trials and Sarcoma Unit, Institut Bergonié, Bordeaux, France; University of Bordeaux, Bordeaux, France; <sup>3</sup>Explicyte Immuno-Oncology, Bordeaux, France



7392

## Background

- Immune exclusion, characterized by a predominance of CD8+ T cells in the stroma of the tumor microenvironment (TME) which are not in contact with tumor cells, is associated with a lack of patient response to immune checkpoint inhibitor therapy.
- Artificial intelligence (AI) models have shown promise in quantifying tissue and cell features from images of hematoxylin and eosin (H&E)-stained slides without the need for immunostaining of cells, but they fall short in identifying specific cell subtypes (e.g. CD8+ T cells vs lymphocytes).
- Here we describe the development of a machine learning model that can classify CD8-based immune phenotypes (IP) using features extracted from H&E images alone.

## Methods

- Slides from 39 non-small lung cancer (NSCLC) and triple-negative breast cancer (TNBC) cases were stained by multiplex IHC (mIHC) for CD8 and pan-cytokeratin (panCK). Pathologist assessment was done to classify the IP of tumors as: desert, with a paucity of CD8+ T cells; excluded, with a preponderance of CD8+ T cells not penetrating the tumor parenchyma; and infiltrated, with abundant CD8+ T cells within the tumor parenchyma.
- Adjacent H&E images were scanned at 40X. AI-powered TME models developed by PathAI (PathExplore™) were deployed for tissue classification and cell type identification, including demarcation of the epithelial-stromal interface.
- 115 morphology-based features extracted from the 25 tumor samples classified as immune excluded (12 NSCLC, 13 TNBC) and the 7 tumor samples classified as immune infiltrated (3 NSCLC, 4 TNBC) were used as input into a machine learning model to identify H&E-derived features most predictive of immune phenotype. Features from the 14 samples classified as desert were not included.
- The feature selection process and immune exclusion score quantification was driven by an ensemble L1-norm support vector machine (Ens-L1-SVM) (Figure 1).
- The trained model was tested in select TCGA cohorts using H&E feature data extracted using an older version of the PathExplore™ models (Diao et al. (2021); PMID: 33712588).

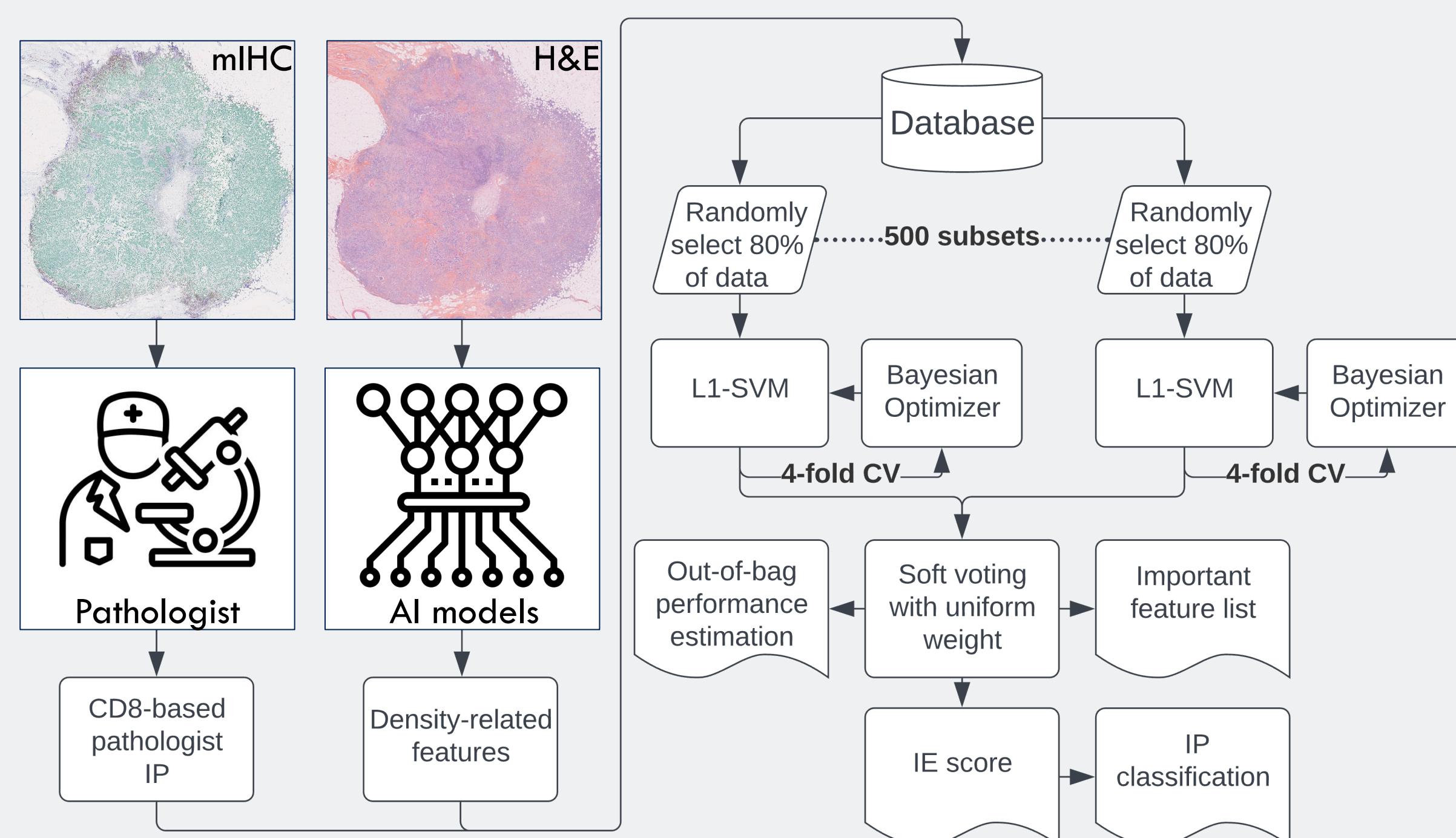


**Figure 1.** An Ens-L1-SVM model was trained using CD8-based immune phenotype classification from mIHC and H&E-derived density-related features.

## Results

- The Ens-L1-SVM model selected 6 H&E features (Table 1) that are predictive of CD8-defined IP with the out-of-bag F1 estimation at 0.93. A coefficient was defined for each feature which represents the direction and degree of contribution of that feature to the IP prediction.

Model-selected H&E Features	Coefficient
Density of fibroblast cells in tumor	1.3
Density ratio of lymphocyte cells in cancer stroma over cancer epithelium	0.6
Density ratio of macrophage cells in cancer stroma over interface	0.5
Density ratio of lymphocyte cells in cancer epithelium over interface	-0.2
Density ratio of cancer epithelial cells in interface over cancer epithelium	-0.6
Density ratio of lymphocyte cells over macrophage cells in cancer epithelium	-1.6



**Table 1.** H&E spatial features selected by Ens-L1-SVM model.

- The trained model was run on H&E feature data from 2740 cases across 5 TCGA cohorts (LUAD, LUSC, BRCA, STAD, SKCM). An IE score and was calculated by the model for each case and an IP assigned

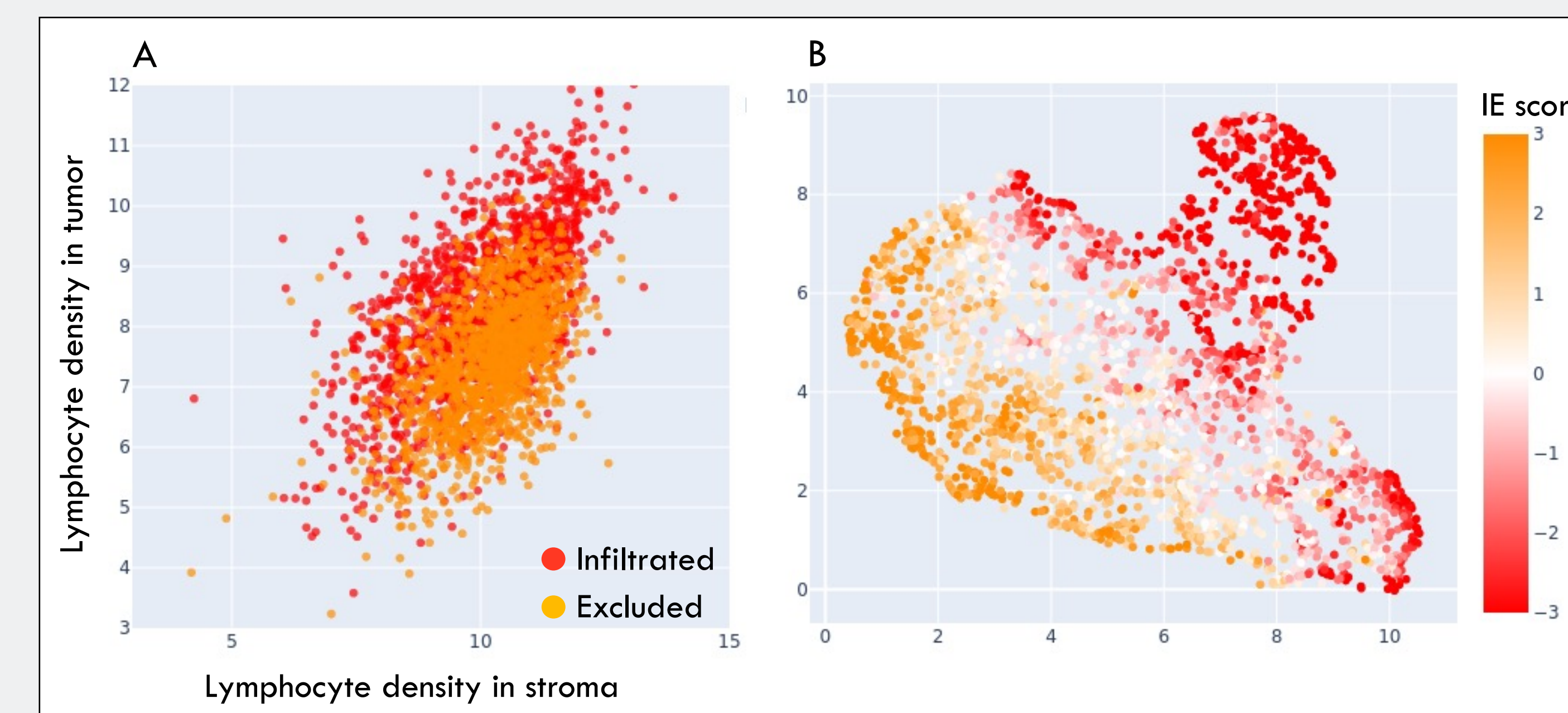


**Figure 3.** Application of the trained model to a TCGA cohort of 2740 samples. A. Scatterplot of the predicted IP by lymphocyte density in tumor and stroma. Samples with positive IE scores are labeled as excluded (yellow), and negative scores as infiltrated (red). B) UMAP of IE score determined from the 6 model-selected features.

- An immune exclusion (IE) score for each sample was calculated in the feature space by the signed distance to the separation hyperplane defined by the Ens-L1-SVM model (Figure 1). Samples with positive IE score are classified as immune-excluded; those with a negative IE score as immune-infiltrated (examples shown in Figure 2).

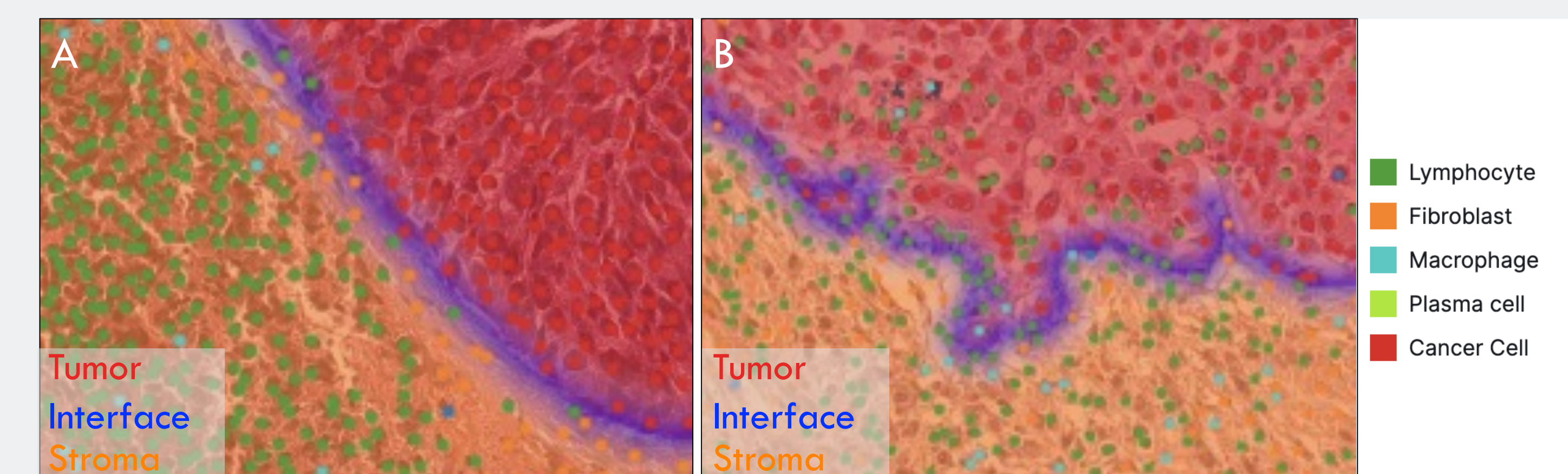


**Figure 2.** Tissue and cell masks overlaid on H&E image from an A) Immune excluded sample (positive IE score); and B) Immune infiltrated sample (negative IE score).

- The IE Score-assigned IP for each TCGA sample does not simply recapitulate the density of lymphocytes in tumor and stroma for each case (Figure 3A), though excluded samples appear to have relatively higher distribution of lymphocytes in stroma relative to tumor. This reflects that the model is not simply predicting the relative location of lymphocytes, but additionally utilizing features of the TME designed to predict CD8-defined immune exclusion.
- UMAP dimensionality reduction (Figure 3B) indicates that the 6 selected features separate TCGA samples into infiltrated and excluded with a clear boundary in between. However, with the lack of reliable CD8 immune phenotype labeling for TCGA, the model performance on the TCGA samples is yet to be validated.

## Conclusions

- The study highlights the effectiveness of utilizing morphologic features extracted from H&E images using AI-powered models as predictors of CD8-defined immune exclusion, providing an option for patient stratification by immune phenotype using widely-available H&E images.
- The model-selected features and direction of association align with prior knowledge of the mechanism or manifestations of immune exclusion or infiltration in the TME, including the relative density of lymphocytes in tumor and stroma.
- While the model demonstrated robust performance on a limited sample size and is anticipated to generalize well due to its linear nature, further validation across diverse datasets and tumor types is crucial for ensuring the reliability and applicability of our findings.

